Glancing angle x-ray diffraction

van Brussel, B. A. ; de Hosson, J. Th. M.

Published in:
Applied Physics Letters

DOI:
10.1063/1.111847

Glancing angle x-ray diffraction: A different approach

B. A. van Brussel and J. Th. M. De Hosson
Department of Applied Physics, Materials Science Centre, University of Groningen, Nijenborgh 4, 9749 AG Groningen, The Netherlands

(Received 5 October 1993; accepted for publication 21 December 1993)

This letter describes a novel technique of diffracted beam glancing angle x-ray diffraction by which depth profiles of stresses and transformed phases in structures like implanted materials can be determined. An important feature is that this method may be applied successfully in a standard powder diffractometer. It is shown that, beside the well-known incident beam glancing angle method which usually requires rather sophisticated equipment with parallel beam optics combined with more intense x-ray sources, diffracted beam glancing angle x-ray diffraction can be applied as well.

Stress measurements by x-ray diffraction represent an evolving field of research, in particular in the domain of integrated circuits where thin film technology is frequently applied. For instance the magnitude and state of stress in the aluminum films is of current interest.[1,2] Other focal points of attention are the stresses originating from the misfit between substrate and deposited layer.[3] Multilayers can be used to study the stress state in layers of the order of 2–3 nm thickness.[4] If the multilayers are very thin, the periodicity of the layers can even serve as a diffraction grating providing information about the detailed thickness and behavior of the layers.

Glancing angle diffraction techniques are used when the information needed lies within a thin top layer of the material. Conventional x-ray diffraction reveals information about a top layer of a thickness in the order of 5–10 μm. In contrast, by employing a glancing angle technique this thickness may be an order of magnitude smaller. Usually a synchrotron x-ray source is preferred for glancing angle diffraction experiments for reasons of a higher intensity and a better angular resolution.[5] However, this letter shows that glancing angle diffraction experiments may also be performed using standard x-ray diffraction equipment.

The common way of performing glancing angle x-ray diffraction is to apply the incident beam at a small angle with the surface of the specimen under investigation.[6–8] This requires a very small divergence of the primary beam or the use of a narrow parallel beam. In this situation the diffracted intensity will be small, requiring long measuring times. The different approach proposed here is letting the diffracted beam make a small angle with the specimen surface. In practice our approach has several advantages, the adjustment of the primary beam does not need any special attention and the divergence of the primary beam may be larger resulting in a higher intensity. In general, the grazing incident method will give a broader spot on the detector than the grazing diffracted method using the same divergence slit. The diffracted beam glancing angle x-ray diffraction technique will be demonstrated by the determination of a depth profile of a bcc layer found in Ne^+ implanted in face-centered-cubic (fcc) Fe (SS304).

In Fig. 1 the general goniometer setup for the two different glancing angle diffraction methods are depicted. The glancing angle β is determined by the diffraction angle θ and the angle ψ in the following way: $\beta=\theta-|\psi|$. The important feature of glancing angle x-ray diffraction is the sensitivity for the top layer of the specimen. This sensitivity depends on the glancing angle used. The path of an x ray through the specimen is depicted in Fig. 2. The path length x can be expressed as

$$x(z)=\frac{2\sin\theta\cos\psi}{\sin(\theta-\psi)\sin(\theta+\psi)}z. \tag{1}$$

Here, z is the penetration depth normal to the specimen surface as depicted in Fig. 2. This equation hold for angles greater than the critical angle. The total x-ray intensity diffracted by a layer of thickness d (taking into account only absorption) is written as

$$\left[\frac{I}{I_0}\right]_{\text{top layer of thickness } d}\approx\int_0^d e^{-(\mu/\rho)\rho x(z)}\,dz, \tag{2}$$

where the integration takes place over the fraction of the intensity of the primary x-ray beam diffracted at depth d. I_0 is the total primary intensity. In fact the right-hand side of Eq. (2) includes a proportionality constant that depends on structure factor, multiplicity, etc. For the moment this is neglected, since here only absorption is taken into account. Although this omission will lead to some error in the determination of the thickness of the body-centered-cubic (bcc) layer, the accuracy of this thickness determination is not very great anyway. Consequently, a possible composition gradient in the depth direction z does not really affect the overall outcome. The mass absorption coefficient μ/ρ is independent

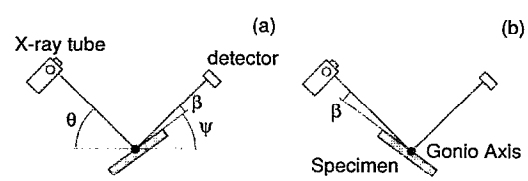

FIG. 1. (a) Diffracted beam glancing angle x-ray diffraction. (b) Incident beam glancing angle x-ray diffraction.

 0003-6951/94/64(12)/1585/3/$6.00

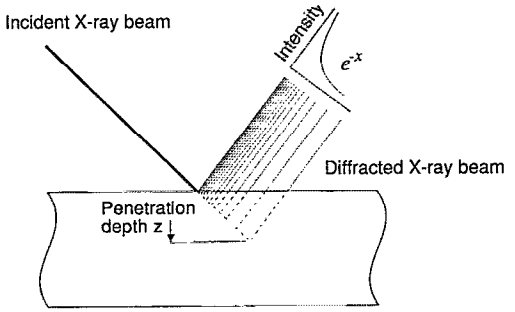

FIG. 2. X-ray path through the specimen. The intensity of the diffracted beam is proportional to e^{-x}. Here, x is the path length of the x ray through the specimen and is related to the penetration depth z.

of the physical and chemical state of the material and is constant at a given wavelength. We now calculate the ratio between the total diffracted intensity that comes from a layer of thickness d and the total diffracted intensity I_{0D}. This implies taking the quotient of two integrals as in Eq. (2) one from 0 to d and the other from 0 to $d_{\max}$. Since the denominator I_{0D} is equal to -1 for $d_{\max}$ becoming infinite, this ratio can be simplified to

$$\frac{I}{I_{0D}} = 1 - \exp\left(-\frac{\mu}{\rho} \frac{2\rho \sin\theta \cos\psi}{\sin(\theta-\psi)\sin(\theta+\psi)} d \right), \tag{3}$$

after substitution of Eq. (1) for $x(d)$. Equation (3), which is actually quite similar to,[9] is depicted in Fig. 3 for one specific set of diffraction conditions: Cu radiation, $\theta=22°$, $\mu/\rho = 27.8\ \mathrm{m^2 kg^{-1}}$, and $\rho = 7.8\times10^3\ \mathrm{kg\ m^{-3}}$. Depending on the value used for ψ, the diffracted x-ray intensity comes from a layer of thickness of only 0.35 to 1.9 μm. These results are valid for both incident beam glancing angle x-ray diffraction and diffracted beam glancing angle x-ray diffraction. The differences between the two methods are found in the irradiated area, and hence in the spot size of the diffracted beam on the detector, and the sensitivity for errors in the goniometer calibration, see Fig. 4.

In Figs. 4(a) and 4(c) the spot size is depicted. In the case of the diffracted beam glancing angle x-ray diffraction

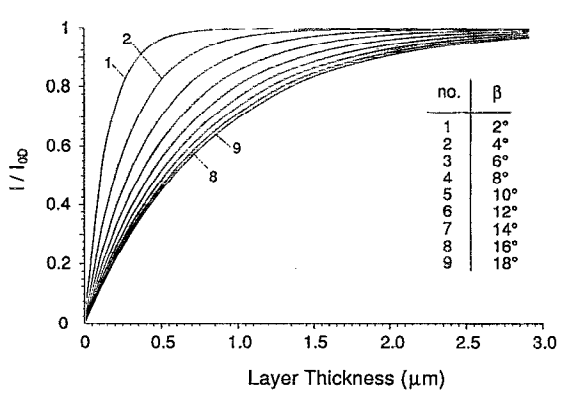

FIG. 3. The fraction of the intensity of the diffracted beam diffracted by a layer vs the layer thickness. $\beta=\theta-|\psi|$.

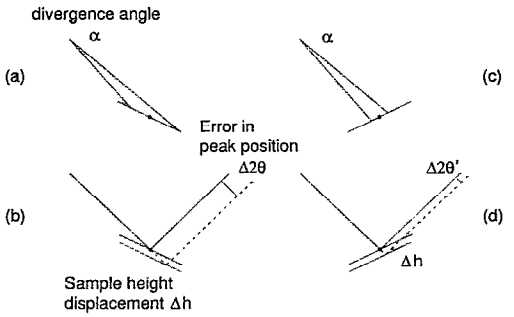

FIG. 4. The influence of the divergence angle upon the irradiated area and of a specimen displacement upon the error in the peak position. On the left for the incident beam glancing angle method and on the right for the diffracted beam glancing angle method.

[Fig. 4(c)] the spot size is an order of magnitude smaller compared to the incident glancing angle x-ray diffraction. Considering the matter of the calibration of the goniometer for the glancing angle x-ray measurements, it is clear from Figs. 4(b) and 4(d) that the specimen height is critical in the case of the incident glancing angle method and noncritical in the case of the diffracted beam glancing angle method. The specimen displacement, defined as Δh in Fig. 4, is in both situations the same. However, the error in 2θ is significantly larger in the case of the incident beam glancing angle method.

The application of the diffracted beam glancing angle x-ray diffraction technique will be illustrated by an example in which Ne^+ is implanted in fcc Fe. The motivation for this study is that ion implantation might be able to reduce or even reverse some unfavorable properties of laser treated materials[10,11] like residual tensile stresses. In fact the shear stress field of inert gas bubbles may induce a local transformation to bcc, provided bubble size and pressure are large enough.[12] The question to be answered is whether this (martensitic) shear transformation indeed nucleates at these bubbles and what are the thickness and depth under the surface of this transformed layer. The specimen investigated was implanted with $2.5\times10^{17}\ \mathrm{Ne^+\ cm^{-2}}$, which is the critical dose for the bcc transformation to occur. The x-ray diffraction experiments were performed on a powder diffractometer Philips PW 1820 fitted with a Cu tube. The diffraction peak used for the measurements is the γ 111 peak, found at 44.6° 2θ. The experiments performed on the specimen consist of scans of the γ 111 peak for several glancing angles β. After performing background correction, the intensities of the peaks are fitted against the theoretical calculated profiles. By subtracting the intensities according to Eq. (3) for two different depths a_1 and a_2 the intensity diffracted by a layer under the surface is obtained. It turned out that the diffraction peaks measured with the diffracted beam glancing angle method are sharper than those measured with the incident beam glancing angle method. A divergence slit of $\frac{1}{4}$ was used for the diffracted beam experiments and a divergence slit of $\frac{1}{12}$ was used for the incident beam experiments, however, the full width at half-maximum is 0.24°, 2θ in the diffracted beam case and 0.7° 2θ in the incident beam case.

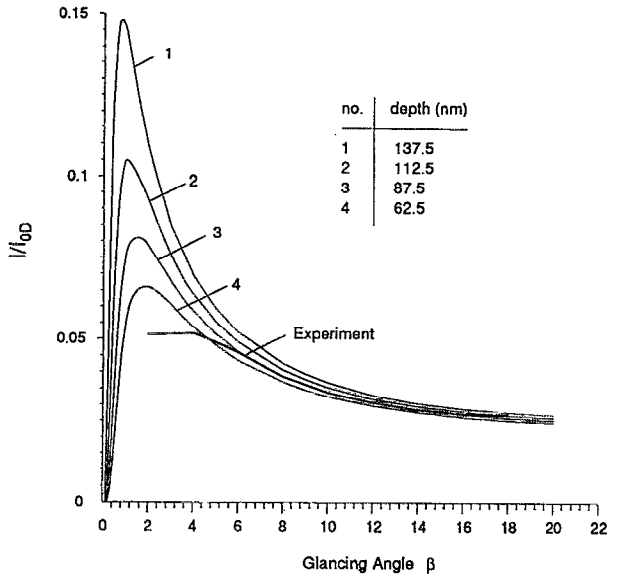

FIG. 5. A fit of the experimental data.

Also visible is the fact that in the case of the incident glancing angle method the sample height is critical. Although adjusted with an accuracy of 0.02 mm a peak shift is present.

In Fig. 5 the results of the diffracted beam glancing angle measurements are fitted against the theoretical curves. If we look at the intensity as a function of glancing angle, it is obvious that in the case of the diffracted beam glancing angle method the intensities obey the theoretically derived results as depicted. The results of the incident beam glancing angle method did not show this behavior. This is most probably caused by the optical arrangement of the x-ray equipment, in particular, the divergence slit.

The following two points should be noted. First, the curve of the experimental data follows the path as calculated for a layer of bcc under the surface. Hence, one conclusion is that the x-ray measurements reveal that the fcc to bcc transformation takes place at the Ne bubbles. The second point to be noted is the quality of the fit. By changing the two depths a_1 and a_2 the thickness and the depth of the bcc layer is determined. The thickness is equal to a_2-a_1, and the depth of the center of the layer is located at $(a_1+a_2)/2$. The curve No. 3 shown in Fig. 5 is the best fit and points at a layer thickness of 25 ± 25 nm located at 87.5 ± 50 nm. The misfit at the lower values of β is explained by noting that the specimen are not entirely flat and the equipment used is not optimally suited for angles in the region below $\beta=2°$.

As a point of discussion we will emphasize that generally speaking there are two possible ways to perform glancing x-ray diffraction. The first and most commonly used is the glancing incident beam x-ray technique. The second way is to perform *diffracted* beam glancing angle diffraction. The diffracted beam glancing angle technique may even be preferred above the incident beam glancing angle technique. First, the width of the irradiated area employing the diffracted beam glancing angle technique is smaller using the same divergence slit. This means that with the incident beam glancing angle technique a smaller divergence angle must be used to obtain an equally sized irradiated area. This leads to a loss of intensity. Second, the glancing angle measurements may be more accurate in the case of the diffracted beam glancing angle technique as the spot size of the diffracted beam on the detector is smaller which leads to a better spatial resolution. Finally, small errors in the alignment of the goniometer axis relative to the x-ray tube have a large effect on the position of the irradiated area on the specimen in the case of the incident beam glancing angle technique and a negligible effect in the case of the diffracted beam glancing angle technique. In the case of the incident beam glancing angle technique this leads to a low accuracy in position determination of the measured diffraction peak.

A different approach to glancing angle x-ray diffraction usable with normal x-ray diffraction equipment is proposed in Ref. 13. Instead of turning the specimen around the axis of the goniometer it is turned around the diffraction vector. The normal θ-2θ diffraction is maintained and by changing the angle around the diffraction vector the penetration depth may be changed, thereby enabling depth distribution experiments. However, compared to the diffracted beam glancing angle method as described in this paper the proposed method in Ref. 13 requires a narrow beam that must very accurately be directed to the cross point of both rotation axes otherwise the results will be inaccurate. In literature some other techniques are reported, grazing-incidence diffraction[14] to characterize surface layers of depths less than 100 nm and rocking curve tails[15] to determine a depth distribution of imperfections. These techniques involve specialized experimental techniques.

In conclusion, this letter describes a novel technique of diffracted beam glancing angle x-ray diffraction by which depth profiles of stresses and transformed phases in structures like implanted materials can be determined. An important feature is that this method may be applied successfully in a standard powder diffractometer. Beside the incident beam glancing angle method which requires rather sophisticated equipment with parallel beam optics combined with more intense x-ray sources, the diffracted beam glancing angle x-ray diffraction can be applied as well.

[1] M. A. Korhonen and C. A. Paszkiet, Scr. Metall. **23**, 1449 (1989).
[2] A. J. Perry, L. Simmen, and L. Chollet, Thin Solid Films **118**, 271 (1984).
[3] A. J. Perry and L. Chollet, J. Vac. Sci. Technol. A **4**, 2801 (1986).
[4] Ph. Goudeau, K. F. Badawi, A. Naudon, and G. Gladyszewski, Appl. Phys. Lett. **62**, 246 (1993).
[5] B. Chu, Y. Li, and T. Gao, Rev. Sci. Instrum. **63**,, 4128 (1992).
[6] C. Li, Z. Mai, S. Cui, and J. Zhou, J. Appl. Phys. **70**, 4172 (1991).
[7] E. D. Specht, C. J. Sparks, and C. J. McHargue, Appl. Phys. Lett. **60**, 2216 (1992).
[8] N. Itoh, Jpn. J. Appl. Phys. **31**, L1140 (1992).
[9] B. D. Cullity, *Elements of X-Ray Diffraction*, 2nd ed. (Addison-Wesley, Reading, MA, 1978), p. 292.
[10] H. DeBeurs and J. Th. M. De Hosson, Appl. Phys. Lett. **53**, 663 (1988).
[11] J. Y. Xu, B. A. v. Brussel, P. M. Bronsveld, and J. Th. M. De Hosson, Surf. Coat. Technol. **45**, 43 (1991).
[12] J. Noordhuis and J. Th. M. De Hosson, Acta Metall Mat. **38**, 2067 (1990).
[13] N. Itoh, Appl. Phys. Lett. **62**, 690 (1993).
[14] V. H. Etgens, R. Pinchaux, M. Sauvage-Simkin, J. Massies, N. Jedrecy, N. Greiser, and S. Tatarenko, Surf. Sci. **251/252**, 478 (1991).
[15] J. M. Baribeau and S. J. Rolfe, Appl. Phys. Lett. **58**, 2129 (1991).